Dyes and Pigments 82 (2009) 196–203

Contents lists available at ScienceDirect

Dyes and Pigments

journal homepage: www.elsevier.com/locate/dyepig

Photophysical characterization of triazole-substituted coumarin fluorophores

Jessie A. Key [a,b], Sherni Koh [b], Qadir K. Timerghazin [b], Alex Brown [b], Christopher W. Cairo [a,b,*]

[a] Alberta Ingenuity Centre for Carbohydrate Science, Department of Chemistry, University of Alberta, Edmonton, Alberta T6G 2G2, Canada
[b] Department of Chemistry, University of Alberta, Edmonton, Alberta T6G 2G2, Canada

ARTICLE INFO

Article history:
Received 9 September 2008
Received in revised form
4 January 2009
Accepted 5 January 2009
Available online 13 January 2009

Keywords:
Fluorescent dye
Triazole
Coumarin
Click chemistry
Absorbance
Fluorescence
Bioconjugate

ABSTRACT

The photophysical properties of fluorochromes are directly influenced by their chemical structure. There is increasing interest in chemical strategies that provide controlled changes to the emission properties of biologically compatible fluorophores. One strategy employed is the conversion of a fluorophore-attached alkyne to a triazole through a copper-catalyzed Sharpless-Meldal reaction. In this study, we have examined a series of structurally related coumarin fluorophores and evaluated changes in their photophysical properties upon conversion from alkyne to triazole forms. Ethynyl-coumarin structures showed increases in quantum yield (ca. 1.2- to- 9 fold) and bathochromic shifts (up to 23 nm) after triazole formation. To extend these results, we tested the ability of time-dependent density functional theory (TD DFT) to predict the observed changes in fluorophore absorption properties. We found excellent correlation between the predicted absorption values and experiment, providing a useful tool in the design of new fluorogenic probes.

1. Introduction

The characterization of biomolecular systems has been revolutionized by concurrent developments in fluorescence spectroscopy and biomolecular labeling strategies. The advent of sensitive fluorescence detectors has enabled advances in biological imaging and the emergence of the field of single molecule spectroscopy. Bioconjugate strategies for the ligation of fluorescent labels to biomolecules have become important for biochemical characterization, as they allow detection of these species in complex mixtures [1], and their diversity provides access to previously intractable systems. The specificity of any labeling strategy is critical to success in biological assays, whether used for research, commercial, or therapeutic purposes. Bioconjugate methods have been applied to proteins, nucleic acids, carbohydrates, lipids and cells [2–7]. However, there remains a need for bioconjugate strategies with improved sensitivity and selectivity.

Chemical reactions that are specific for a single functional group in the presence of other biomolecules are termed *bioorthogonal reactions*. Bioorthogonal reactions must be tolerant of aqueous solvent conditions and the presence of functional groups such as amines, alcohols, and carboxylic acids. Successful examples provide non-perturbing chemical handles for the modification of biomolecules in vitro or in vivo with exogenous probes [8]. A currently popular example of this class of reactions is the Sharpless–Meldal reaction, which couples azides and alkynes through a Cu(I)-catalyzed Huisgen 1,3-dipolar cycloaddition [8–12]. The high selectivity and reactivity of the azide and alkyne groups, mild aqueous reaction conditions, and small size of the functional groups make this reaction ideal for many biological applications [11,13].

Traditionally, the Huisgen 1,3-dipolar cycloaddition between azides and alkynes is performed at high temperatures and long durations [14]. Generally, electron deficient alkynes exhibit good regioselectivity, while other alkynes give mixtures of 1,4- and 1,5-triazole regioisomers [11,14]. The Cu(I)-catalyzed form of the reaction uses much milder conditions and is known as the Sharpless–Meldal reaction [9,10]. The reaction has been employed in numerous biochemical studies to detect binding partners, enzymes and substrates, or engineered proteins [15–18].

The product of the Sharpless–Meldal reaction is a triazole moiety which has been proposed to provide a means to alter the spectral properties of the initial azide or alkyne. Known examples include attachment of the azide or the alkyne to the fluorophore core [19–23]. Subsequent formation of the triazole leads to varying increases in emission intensity and changes in emission wavelength, properties desirable in fluorogenic probes. Combinatorial approaches to identify new fluorophores have been employed to

* Corresponding author. Alberta Ingenuity Centre for Carbohydrate Science, Department of Chemistry, University of Alberta, Edmonton, Alberta T6G 2G2, Canada. Tel.: +1 780 492 0377; fax: +1 780 492 8231.
E-mail address: ccairo@ualberta.ca (C.W. Cairo).

0143-7208/$ – see front matter © 2009 Elsevier Ltd. All rights reserved.
doi:10.1016/j.dyepig.2009.01.001

identify suitable substrates [19]. It is notable that even small changes to these structures can have a significant impact on the resulting emission properties. For example, switching the attachment point on the fluorochrome from the N1 to the C4 position of the triazole can result in significant differences in emission properties [21].

Substitution of coumarin fluorophores with azide or alkyne groups is known to induce changes in fluorescence properties. The 3- and 7-positions of the coumarin backbone have been shown to strongly modulate fluorescence by affecting the energy of the molecule's two lowest excited states [19,20]. This property has been used extensively for detection of enzymatic activity by substitution at the 7-position, exploiting the increase in emission upon unmasking of a hydroxycoumarin [24–27]. Conjugation of an electron-donating triazole ring to the coumarin backbone at one of these positions causes an increase in quantum yield and a bathochromic shift in emission relative to the starting alkyne [19–22]. This observation was first reported by Sivakumar and colleagues with a series of eight 3-azido substituted coumarins [19]. Zhou and Fahrni examined the influence of triazole formation on a single 7-ethynyl substituted succinic acid coumarin ester [20]. Applications of triazole structures to fluorogenic probe strategies have capitalized on an increase in fluorescence emission to enhance signal to noise in labeling and imaging experiments. Recent examples have favored the use of 3-azido-7-hydroxy coumarin in the labeling of proteins, DNA, and glycoconjugates [19,20,22,28–30]. Although this fluorophore shows a large increase in quantum yield (QY, Φ) upon triazole formation, hydroxycoumarins are environmentally sensitive due to the acidic hydroxyl group [24,31,32]. Therefore, quantitative use of these dyes can be complicated by pH sensitivity to the biological microenvironment [7,24,31]. Ethynyl substitutions of these structures can, therefore, provide an alternative strategy that avoids pH sensitivity [20].

In this study, we undertook a systematic examination of changes to fluorescent properties among a group of related fluorophore backbones. We chose to examine coumarin fluorophores since similar structures have been used successfully in fluorogenic strategies. These derivatives are synthetically accessible by established precedents for introduction of alkyne or azide groups onto the coumarin structure at the 3- [19,29,30], 4-[33] and 7-positions [20]. We sought to examine the modulating effects of conjugated triazole formation on this series of ethynyl-coumarin and benzocoumarin structures for changes in UV–vis absorbance, quantum yield, molar absorption coefficient, and fluorescence emission. Comparison of the experimental data with theoretical calculations of the absorbance properties of the fluorophores allowed us to test the accuracy of electronic models.

2. Results and discussion

2.1. Fluorophore synthesis

Synthesis of the pre- and post-click compounds used in this study was performed using established methods, as depicted in Fig. 1. Coumarin fluorophores were generated by Pechman and Knoevenagel condensations of the corresponding diols, generating four different hydroxycoumarins. To generate the 7-hydroxy-4-methyl coumarin backbone (**1a**, 4-methylumbelliferone), resorcinol (**5**) was reacted with ethyl acetoacetate in a $TiCl_4$-catalyzed Pechmann condensation [34]. Two isomers of benzocoumarin were generated from 2,7-dihydroxynapthalene (**6**) in a sulfuric acid-catalyzed Pechmann condensation with ethyl acetoacetate, providing the angular- (**2a**) and linear-benzocoumarins (**3a**) after purification [35–37]. A second umbelliferone derivative was generated by a piperidine catalyzed Knoevenagel condensation of diethyl glutaconate with 2,4-dihydroxybenzaldehyde to form compound **4a** [38]. The hydroxyl derivatives (**1a**–**4a**) were then converted to the corresponding triflic ethers. The intermediate triflate was used without purification to generate trimethylsilyl-protected alkyne intermediates via Pd(0)-catalyzed Sonogashira coupling with trimethylsilyl acetylene [20,39]. Deprotection with tetrabutylammonium fluoride (TBAF) resulted in the ethynyl compounds (**1b**–**4b**) [20].

With the conjugated alkyne derivatives in hand, we proceeded to generate the click products to characterize their properties. Although an azide coupling partner that is itself conjugated to an aromatic moiety could enhance the fluorogenic properties of the products [19], we chose to use benzylazide to more closely mimic a triazole product that might be formed in a bioconjugate addition. A variety of conditions have been used for similar reactions, with variables including the choice of base/ligand, solvent, reducing agent, and source of copper [14]. The triazolyl-click products (**1c**–**4c**) were generated using two sets of conditions, in the first, Cu(I) catalyzed Sharpless–Meldal reaction with benzylazide was performed using CuI in 1:1 methanol/water with triethylamine as base [14]. These reactions proceeded in good to moderate yields (44–87%). However, we observed minor amounts of the 5,5′-bistriazole products under these conditions, as evidenced by the appearance of a new ^{1}H NMR signal between 4 and 5 ppm and the observation of a peak in the mass spectrum for [$2M^+$-2H] [40]. In one case, we were successful in obtaining crystals of the side product suitable for X-ray diffraction [41]. This contaminant was only observed in detectable amounts in the synthesis of **1c** (23% of bistriazole) and **4c** (7% of bistriazole). We obtained exclusive formation of the desired products **1c** and **4c** with good yields (ca. 62–79%) by altering the conditions used for these substrates to 0.2 equiv. $CuSO_4$ and 0.3 equiv. ascorbic acid in 1:1 methanol/water (Fig. 1). In reactions with equimolar $CuSO_4$ and ascorbic acid at pH 4, we observed the formation of a fluorescent contaminant. The contaminant could be generated in the absence of the alkyne derivative and showed fluorescent emission at 450 nm. The triazole compounds were, therefore, purified by flash chromatography before characterization.

2.2. Fluorophore characterization

To quantitate changes in photophysical properties after triazole formation, we characterized the properties of the hydroxyl- (**1a**–**4a**), ethynyl- (**1b**–**4b**), and triazolyl- (**1c**–**4c**) compounds. These compounds were characterized to determine their UV–vis absorbance spectra, fluorescence emission, molar absorption coefficients, and quantum yields (Table 1). Spectral characterization was performed in ethanol at pH 7 using a quinine sulfate standard in 0.5 M sulfuric acid [31,42]. Our results confirmed that triazole formation generally enhances the fluorescence of alkyne derivatives and can induce shifts in emission wavelength (Table 1). In all four alkynes we observed a large decrease in QY relative to the starting hydroxyl derivatives (ca. 20–90%) with **1b** (from 0.33 to 0.02) and **3b** (from 0.35 to 0.01) showing the most significant changes. Three of the alkyne structures (**1b**, **3b**, and **4b**) show a significant increase in extinction coefficient relative to the hydroxyl derivatives. Conversion of the alkyne structures to the corresponding triazole increased the QY of all structures, with **1c** and **3c** showing the largest relative changes. With the exception of compound **2b**, triazole formation caused a slight decrease in the extinction coefficients as compared to the corresponding alkyne. The increased brightness ($\varepsilon \times \Phi$, $cm^{-1}M^{-1}$) of compounds **1c** and **2c** suggests that these may be the most suitable as fluorogenic probes, while compounds **3c** and **4c** show only minor changes by this analysis. Although relatively large bathochromic shifts have been reported for related compounds, we only observed modest

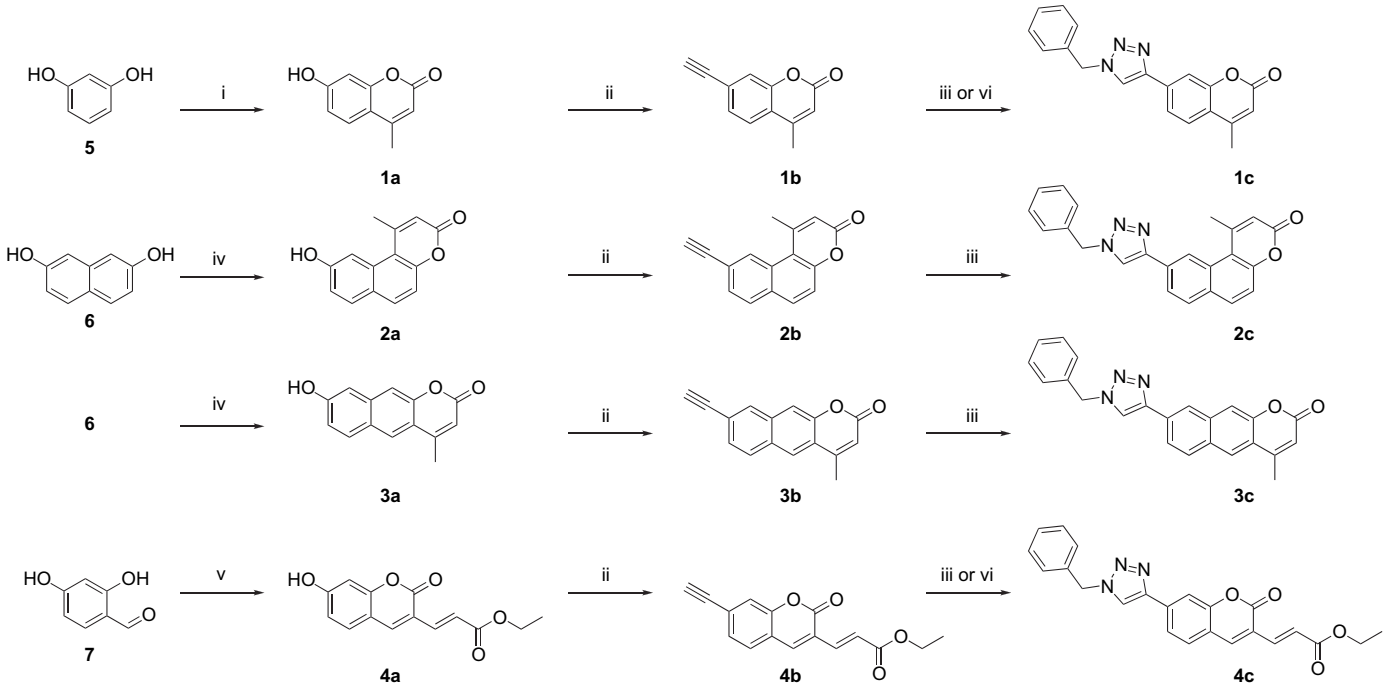

Fig. 1. Synthetic scheme for the generation of click substrates and fluorophores. Reagents and conditions: (i) ethyl acetoacetate, $TiCl_4$, rt, 5 min; (ii) (a) $PhN(SO_2CF_3)_2$, DIPEA, CH_3CN, rt, 30 min; (b) TMS acetylene, CuI, $Pd(PPh_3)_4$, DIPEA, CH_3CN, rt, 48 h; (c) TBAF, MeOH, 60 °C, 30 min; (iii) benzylazide, CuI, TEA, MeOH/H_2O, rt, 2–24 h; (iv) ethyl acetoacetate, 80% H_2SO_4, rt, 24 h; (v) diethyl glutaconate, EtOH, piperidine, reflux 89 °C, 24 h; (vi) $CuSO_4$, ascorbic acid, EtOH/H_2O, rt, 2–7 d.

changes in emission wavelength upon triazole formation, with the largest of these seen in compounds **2c** (17 nm) and **4c** (23 nm) (Fig. 1b) [20].

Although previous studies have suggested that triazole formation on conjugated alkyne fluorophores can induce large increases in fluorescence, we found that this trend is highly dependent on the fluorophore backbone. Several of the coumarin-based fluorophores examined here showed substantial increase in brightness upon triazole formation, and could prove useful as biological probes. The results obtained demonstrate that the impact of substitutions on the fluorophore backbone must be carefully considered. It is worth noting that hydroxycoumarin structures are often assessed at higher pH where their anionic forms are more prevalent. Replacement of the hydroxyl group with an alkyne, triazole, or methoxy group reduces the emission of the fluorophore as a result [20,25,43]. We examined the properties of our fluorophores at high pH and confirmed they were similar to neutral conditions. Therefore, while dyes that take advantage of this design suffer from reduced brightness, they are conversely less environmentally sensitive.

We found that the alkyne–triazole fluorogenic strategy manifests a variety of effects in each of the backbones studied. The largest increases in total fluorescence emission were seen in series **1** and **3**, with increases in QY between 1.2- and 9-fold. When the brightness of the fluorophore is considered, series **1** and **2** show large increases of 7- and 9-fold, respectively. The intensity of emission is not the only consideration for fluorogenic strategies,

Table 1
Photophysical characterization of compounds.

Compound	Experimental							Theoretical		
	Abs λ_{Max} (nm)	Emission λ_{Max} (nm)	ϵ Absorption coefficient ($cm^{-1}\,M^{-1}$)	Φ Quantum yield[b]	$\Delta\Phi$ $b \rightarrow c$ (%)	$\epsilon \times \Phi$ Brightness ($cm^{-1}\,M^{-1}$)	Δ Brightness $b \rightarrow c$ (%)	Abs λ_{Max} (nm)	Corrected Abs λ_{Max} (nm)[a]	f[e]
1a	323	380	11,600	0.33[c]	850	3800	680	302	324	0.44
1b	325	380	22,000	0.02		440		309	328	0.54
1c	329	381	17,500	0.17		3000		318[d]	333	0.69
2a	*350*	*450*	*13,800*	*0.30*	*120*	*4100*	*890*	*351*	*354*	*0.33*
2b	*362*	*403*	*3,100*	*0.23*		*710*		*346*	*350*	*0.41*
2c	*352*	*420*	*18,000*	*0.35*		*6300*		*349*[d]	*352*	*0.48*
3a	357	466	7,400	0.35	200	2600	140	365	362	0.19
3b	334	437	16,300	0.01		160		329	340	0.53
3c	339	445	11,600	0.02		230		335[d]	344	0.49
4a	*367*	*430*	*11,400*	*0.52*	*120*	*5900*	*50*	*353*	*355*	*1.11*
4b	*360*	*412*	*18,000*	*0.36*		*6500*		*360*	*359*	*1.24*
4c	*358*	*435*	*7,700*	*0.44*		*3400*		*370*[d]	*365*	*1.38*

[a] The corrected values were obtained based on the linear correlation (eq. (1)).
[b] Spectra were obtained in ethanol (pH 7), quantum yields were determined using quinine sulfate as a standard in 0.5 M H_2SO_4 [31,42].
[c] The quantum yield of **1a** was found to agree to within 11% of literature values in ethanol at pH 10 [24,32].
[d] For triazole-substituted coumarins, lower-energy 1,4-isomers were used for calculations.
[e] Oscillator strength.

shifts in emission wavelength can be used to enhance the selectivity of detection. We found that the 3-substituted coumarin backbone in series **4** showed the largest shift in emission wavelength (Fig. 2b), similar to previous reports [20]. Although the shift in λ_{Max} is small in the other derivatives, even these compounds could be used as suitable probes through judicious choice of excitation and emission filters. For example, the tail region of the emission spectra for these compounds (~450–600 nm) can show substantial differences between the alkyne and triazole (Fig. 2a).

2.3. Theoretical prediction of fluorophore absorption

To guide the design of future fluorogenic probes, we explored theoretical methods to predict the properties of alkyne- and triazole-conjugated coumarin fluorophores. Computational quantum chemistry methods are readily available; however, careful testing of the performance of any method is necessary before it can be applied to a particular class of fluorophores. Here, we used the experimental data presented in Table 1 to benchmark the performance of time-dependent density functional theory [44] (TD DFT) in the determination of absorption wavelengths for coumarins. TD DFT is one of the most widely used single-reference approaches to model excited states of organic molecules [45]. Prediction of the fluorescence wavelengths is a significantly more challenging task compared to the absorption properties; thus, we postpone the presentation of computational modeling of the emission of the substituted coumarins to future work.

The calculated absorption wavelengths listed in Table 1 correspond to the transitions with the largest oscillator strengths (*f*) for coumarins in ethanol solution [46]. These were also considered to be bright excited states and correspond to $\pi \rightarrow \pi^*$ type transitions (normally HOMO to LUMO). In most cases, these transitions are to the lowest-energy bright excited states ($S_0 \rightarrow S_1$); in the case of **3b** and **3c**, S_1 had a much smaller oscillator strength when compared with S_2 (0.12 and 0.21 vs. 0.53 and 0.49, respectively). Therefore, for these two structures we chose the next higher excited state (S_2) to correlate with the experimentally observed absorption bands giving rise to fluorescence, omitting the lowest-energy excited state, S_1. The calculated absorption wavelengths significantly deviate from the experimental data, with mean absolute error (MAE) of 13.6 nm. Thus, it is not advisable to use the TD DFT calculated values directly in order to predict the absorption wavelengths. However, we found that there is a good linear correlation between the calculated and experimental absorption λ_{Max} values ($R^2 = 0.936$, Fig. 3):

$$\lambda_{Max}^{exptl} = 140.0 + 0.6082\lambda_{Max}^{calc} \quad (1)$$

This correlation can be used to correct the computed values. Indeed, when the corrected values are used (Table 1), the MAE decreases to 5.3 nm. Similar correlations have been reported [47]; however, this is the first study to include experimental data for alkyne- and triazole-substituted species and anionic forms of the hydroxycoumarins.

It has been proposed that the lower fluorescence quantum yields of the alkyne- vs. triazole-substituted coumarins can be explained by the predominance of the intersystem crossing from the lowest lying singlet state (S_1) to a low lying $(n\pi^*)^3$ triplet state [20]. Indeed, semi-empirical calculations [20] suggest that for alkyne-substituted coumarins the triplet state is lower in energy than the singlet, and this difference is responsible for the higher fluorescence quantum yields of the triazole. However, higher-level TD DFT calculations performed in this work suggest that for the majority of the alkyne-substituted coumarins the $(n\pi^*)^3$ triplet state is also significantly (ca. 0.5 eV) higher in energy than the S_1 state at the ground state equilibrium geometry. Thus, alternative mechanisms of the fluorescence quantum yield enhancement for triazole- vs. alkyne-substituted coumarins may be involved.

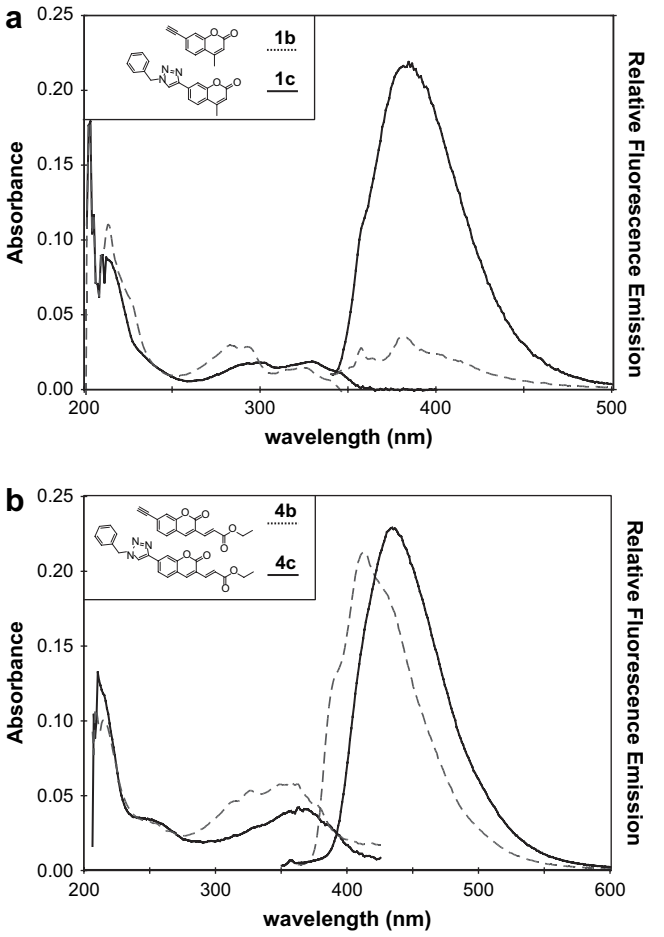

Fig. 2. Absorbance and relative fluorescence emission of alkyne and triazole structures (a) **1b**, **1c** and (b) **4b**, **4c**. Spectra were obtained at equimolar concentrations in EtOH (pH 7) with an excitation wavelength of 325 nm.

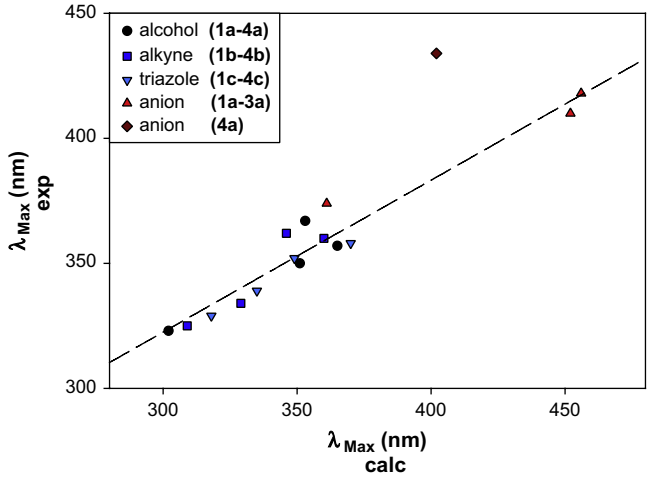

Fig. 3. Correlation of experimental and theoretical absorbance values calculated with PCM-TD-PBE0/6-31 + G(d) method, $R^2 = 0.936$. Note that anion values for compounds **1a**, **2a**, and **3a** are included, whereas the anion of **4a** was excluded. Exclusion of all anionic forms gives $R^2 = 0.827$ [56].

3. Conclusions

The fluorophores used here may be useful for fluorogenic labeling strategies in bioconjugate chemistry. The excitation wavelengths for the triazole structures range from 330 to 370 nm, similar to that of commonly employed dyes such as DAPI and Hoescht [48]. The triazole dyes generated for this study leave room for improvement to become optimal fluorogenic probes. The brightness of all fluorophores studied is low compared to many common dyes, primarily due to their reduced extinction coefficients. We demonstrate here that absorbance wavelength can be accurately predicted for a range of coumarin-based structures, including triazole- and alkyne-containing compounds. Employing rational design and computational prediction, future generations of fluorophores will be tuned to specific applications. We are currently exploring the utility of the fluorophores described for the labeling of biomolecules, and we continue to develop structurally related dyes with improved characteristics.

4. Experimental

4.1. General

Reagents were reagent grade from Sigma–Aldrich (Oakville, Ont) and used without additional purification. Proton and carbon NMR were performed on Varian 300, 400, or 500 MHz instruments at room temperature as noted. Deuterated solvents were obtained from Cambridge Isotope Laboratories (Andover, MA). CD_3OD, $(CD_3)_2SO$, and $CDCl_3$ solvent peaks (3.31, 2.50, and 7.26 for ^1H; 49.0, 39.5, and 77.2 for ^{13}C, respectively) were used as internal chemical shift references. Some spectra contain small amounts of contaminating solvents [49]. Mass spectrometry was performed using an MS50G positive electron impact instrument from Kratos Analytical (Manchester, UK) and a Mariner Biospectrometry positive ion electrospray instrument from Applied Biosystems (Foster City, CA).

4.2. Spectroscopy

Absorbance spectra for all compounds were collected at room temperature with a Hewlett–Packard (Palo Alto, CA) model 8453 diode array UV–vis spectrophotometer. Absorbance measurements were taken using Eppendorf (Hamburg, Germany) UVette cuvettes (220–1600 nm). Fluorescence spectra for all compounds were collected at room temperature with a Photon Technology International model MP1 steady-state fluorimeter. Fluorescence measurements were taken using NSG Precision Cells (Farmingdale, NY) ES quartz cuvettes (190–2000 nm).

4.3. Quantum chemistry calculations

TD DFT calculations were performed using parameter-free Perdew, Burke and Ernzerhof (PBE0) hybrid functional [50] and the standard 6-31 + G(d) basis set [51], as implemented in the Gaussian03 program package [52]. Ground state geometry optimizations for the coumarins were performed at the PBE0/6-31 + G(d) level, and the solvent (EtOH) effects were included using an IEF-PCM polarizable continuum model [53,54].

4.4. General synthesis of trifluoromethanesulfonic acid ester intermediates

Hydroxy compound (**1a**–**4a**) (1 equiv.) and *N*-phenyl bistrifluoromethane sulfonimide ($PhN(SO_2CF_3)_2$, 1.3 equiv.) were added to an oven dried round-bottomed flask and dissolved in acetonitrile (approximately 0.3 M). *N*,*N*-Diisopropylethylamine (DIPEA, 1.3 equiv.) was then added by syringe, briefly turning the solution dark orange. The reaction was allowed to stir for approximately 1–2 h. The reaction mixture was then diluted with EtOAc, washed with water and dried over $MgSO_4$. The compound was concentrated in vacuo and carried forward without further purification.

4.5. General synthesis of trimethylsilanylethynyl intermediates

Trifluoromethanesulfonic acid ester intermediates (1 equiv.) were dissolved in acetonitrile (approximately 0.4 M). $Pd(PPh_3)_4$ (0.1 equiv.) was then added, giving the reaction mixture a light brown colour. CuI (0.2 equiv.) was added, turning the reaction mixture dark brown/black. Trimethylsilyl acetylene (5 equiv.) and DIPEA (3.77 equiv.) were then added to the reaction mixture. The solution was degassed by three freeze/thaw cycles and allowed to stir for 48 h. The reaction mixture was then diluted with EtOAc, washed with NH_4Cl and dried over $MgSO_4$. The crude product was concentrated in vacuo, and purified by gradient flash column chromatography (EtOAc/hexanes).

4.6. General synthesis of ethynyl profluorophores (*1b*–*4b*)

Trimethylsilanylethynyl intermediates (1 equiv.) were dissolved in MeOH (approximately 0.03 M) and heated to 60 °C. Tributylammonium fluoride (TBAF, 3 equiv.) was then added dropwise, and the reaction was allowed to stir for 15 min, turning dark brown. The reaction was quenched with distilled water and filtered; the filtrate then formed a white precipitate under reduced pressure. The precipitate was filtered to give crude product, and was purified by gradient flash column chromatography (EtOAc/hexanes).

4.7. Synthesis of azidomethylbenzene (benzylazide)

Bromomethylbenzene (0.7 mL, 5.85 mmol, 1 equiv.) was dissolved in 15 mL of DMSO, followed by addition of sodium azide (0.57 g, 8.8 mmol, 1.5 equiv.). The reaction mixture was heated to 40 °C, then quenched after 1 h with distilled water. Extraction was performed with diethyl ether, followed by water and brine washes. The organic layer was dried over $MgSO_4$ and concentrated in vacuo. Proton NMR data matched with that of previously reported [55].

4.8. General synthesis of click reaction products (*1c*–*4c*)

The alkynyl compounds (**1b**–**4b**, 1 equiv.) and benzylazide (4–5 equiv.) were dissolved in a 1:1 solution of methanol:water (0.02 M). CuI (0.2 equiv.) was then added, followed by triethylamine (TEA, 2 equiv.). The reaction proceeded at room temperature and was monitored by thin layer chromatography. Reactions were usually completed within 2–48 h. The crude product was concentrated in vacuo, extracted with chloroform and purified by flash column chromatography (CH_2Cl_2/MeOH). In some cases these conditions showed formation of the 5,5′-bistriazole side product (<25%) as evidenced by an additional resonance in the ^1H NMR spectrum between 4 and 5 ppm [40]. To avoid this side product, alternative conditions were used as follows: The alkynyl compounds (**1b** and **4b**) (1 equiv.) and benzylazide (4–5 equiv.) were dissolved in a 1:1 solution of methanol:water (0.03 M alkyne). $CuSO_4$ (0.2 equiv.) and ascorbic acid (0.3 equiv.) were then added, and the reaction was allowed to proceed at room temperature. Reactions were sluggish, and required 2–7 d. The crude product was concentrated in vacuo, extracted with chloroform and purified by flash column chromatography (CH_2Cl_2/MeOH).

*4.8.1. 7-Hydroxy-4-methyl-chromen-2-one (7-hydroxy-4-methyl coumarin) (**1a**) [34]*

Resorcinol (4 g, 36.32 mmol, 1 equiv.) was added to an oven dried round-bottomed flask, and dissolved in ethyl acetoacetate (7 mL, 54.48 mmol, 1.5 equiv.). $TiCl_4$ (2 mL, 18.16 mmol, 0.5 equiv.) was then added by pipette, driving the reaction to completion in moments. The reaction was quenched with water, forming a yellow precipitate. The water was then decanted off, and the precipitate recrystallized in EtOH. Obtained in 97% yield. ^{1}H NMR (300 MHz, DMSO): δ 10.50 (s, 1H), 7.57 (d, 1H, $^3J = 8.7$ Hz), 6.78 (dd, 1H, $^3J = 8.7$ Hz, $^4J = 2.4$ Hz), 6.68 (d, 1H, $^4J = 2.3$ Hz), 6.10 (s, 1H), 2.35 (s, 3H). EI-MS calculated for $C_{10}H_8O_3$: 176.0474; observed: 176.0474: C 68.18, H 4.58; found: C 67.76, H 4.25. $R_f = 0.5$ (9:1 CH_2Cl_2/MeOH).

*4.8.2. 9-Hydroxy-1-methyl-benzo[f]chromen-3-one (**2a**) and 8-hydroxy-4-methyl-benzo[g]chromen-2-one (**3a**) [36,37]*

2,7-Dihydroxynapthalene (4.8 g, 29.44 mmol, 1 equiv.) was dissolved in ethyl acetoacetate (9.4 mL, 73.6 mmol, 2.5 equiv.) and approximately 30 mL of 80% sulfuric acid was added dropwise. The reaction was allowed to stir for 24 h under argon. The reaction was then quenched with water, and the resulting precipitate was filtered. The precipitate was then dissolved in EtOH, filtering off the insoluble material, and concentrated in vacuo. The concentrated solid was then dissolved in 10% NaOH (aq) and the insoluble material was filtered, acidified and recrystallized with EtOH to obtain the white crystalline linear benzocoumarin (**3a**). The filtrate was then acidified with concentrated HCl to pH 1 and allowed to crystallize at 4 °C, yielding the yellow angular benzocoumarin solid.

(**2a**) Obtained in 5.9% yield. ^{1}H NMR (400 MHz, DMSO): δ 10.13 (s, 1H), 8.03 (d, 1H, $^3J = 8.8$ Hz), 7.99 (s, 1H), 7.89 (d, 1H, $^3J = 8.8$ Hz), 7.27 (d, 1H, $^3J = 8.8$ Hz), 7.12 (d, 1H, $^3J = 8.8$ Hz), 2.85 (s, 3H). EI-MS calculated for $C_{14}H_{14}O_3$: 226.0630; observed: 226.0632. $R_f = 0.67$ (10:1 CH_2Cl_2/MeOH).
(**3a**) Obtained in 9.7% yield. ^{1}H NMR (300 MHz, DMSO): δ 10.17 (s, 1H), 8.27 (s, 1H), 7.94 (d, 1H, $^3J = 9.0$ Hz), 7.60 (s, 1H), 7.16 (d, 1H, $^4J = 2.4$ Hz), 7.10 (d, 1H, $^3J = 9.0$ Hz), 6.33 (d, 1H, 1.2 Hz), methyl overlapping DMSO ~2.5 (3H). EI-MS calculated for $C_{14}H_{14}O_3$: 226.0630; observed: 226.0631. $R_f = 0.73$ (9:1 CH_2Cl_2/MeOH).

*4.8.3. 3-(7-Hydroxy-2-oxo-2H-chromen-3-yl)-acrylic acid ethyl ester (**4a**) [38]*

2,4-Dihydroxybenzaldehyde (300 mg, 2.18 mmol, 1 equiv.) was dissolved in approximately 6 mL of ethanol. Diethyl glutaconate was then added (0.40 mL, 2.29 mmol, 1.05 equiv.), followed by 3 drops of piperidine. The reaction mixture was refluxed at 89 °C for 24 h, then cooled to room temperature providing a yellow precipitate, that was then filtered. Obtained in 67% yield (**4a**). ^{1}H NMR (300 MHz, CD_3OD): δ 8.14 (s, 1H), 7.56 (dd, 1H, $^3J = 16.5$ Hz, $^4J = 0.6$ Hz), 7.52 (d, 1H, $^3J = 8.6$ Hz), 6.92 (d, 1H, $^3J = 16.5$ Hz), 6.80 (dd, 1H, $^3J = 8.6$ Hz, $^4J = 2.4$ Hz), 6.71 (d, 1H, $^4J = 2.4$ Hz, $^4J = 0.6$ Hz), 4.23 (q, 2H, $^3J = 6.9$ Hz), 1.31 (t, 3H, $^3J = 6.9$ Hz). EI-MS calculated for $C_{14}H_{12}O_5$: 260.0685; observed: 260.0687: C 64.61, H 4.65; found C 64.78, H 4.49. $R_f = 0.49$ (1:1 EtOAc/hexanes).

*4.8.4. 7-Ethynyl-4-methyl-chromen-2-one (**1b**)*

Obtained in 31% yield over three steps from **1a**. ^{1}H NMR (400 MHz, DMSO): δ 7.75 (d, 1H, $^3J = 8.1$ Hz), 7.49 (d, 1H, $^4J = 1.5$ Hz), 7.44 (dd, 1H, $^3J = 8.1$ Hz, $^4J = 1.6$ Hz), 6.42 (d, 1H, $^4J = 1.2$ Hz), 4.48 (s, 1H), 2.41 (d, 3H, $^4J = 1.3$ Hz). APT ^{13}C NMR (100 MHz, DMSO): δ 159.1, 152.5, 152.4, 127.3, 125.6, 124.7, 119.9, 119.1, 114.8, 83.7, 82.0, 17.7. EI-MS calculated for $C_{12}H_8O_2$: 184.0524; observed: 184.0524: C 78.25, H 4.38; found C 78.00, H 4.51. $R_f = 0.37$ (1:3 EtOAc/hexanes).

*4.8.5. 9-Ethynyl-1-methyl-benzo[f]chromen-3-one (**2b**)*

Obtained in 15% yield over three steps from **2a**. ^{1}H NMR (600 MHz, $CDCl_3$): δ 8.77 (s, 1H), 7.95 (d, 1H, $^3J = 8.9$ Hz), 7.86 (d, 1H, $^3J = 8.4$ Hz), 7.61 (dd, 1H, $^3J = 8.3$ Hz, $^4J = 1.4$ Hz), 7.49 (d, 1H, $^3J = 8.9$ Hz), 6.40 (d, 1H, $^4J = 1.1$ Hz), 3.23 (s, 1H), 2.95 (s, 3H). APT ^{13}C NMR (100 MHz, $CDCl_3$): δ 159.9, 154.9, 153.5, 133.1, 130.9, 129.8, 129.6, 129.1, 128.1, 121.5, 118.7, 116.9, 114.2, 83.7, 78.7, 26.2. EI-MS calculated for $C_{16}H_{10}O_2$: 234.0681; observed: 234.0682. $R_f = 0.39$ (1:3 EtOAc/hexanes).

*4.8.6. 8-Ethynyl-4-methyl-benzo[g]chromen-2-one (**3b**)*

Obtained in 14% yield over three steps from **3a**. ^{1}H NMR (600 MHz, $CDCl_3$): δ 8.07 (s, 1H), 8.04 (s, 1H), 7.89 (d, 1H, $^3J = 8.6$ Hz), 7.67 (s, 1H), 7.53 (dd, 1H, $^3J = 8.5$ Hz, $^4J = 1.5$ Hz), 6.37 (d, 1H, $^4J = 1.3$ Hz), 3.24 (s, 1H), 2.56 (s, 3H). APT ^{13}C NMR (100 MHz, $CDCl_3$): δ 160.2, 151.4, 150.6, 133.9, 131.4, 129.2, 128.5, 128.3, 124.7, 121.8, 120.7, 116.2, 112.7, 83.3, 79.1, 18.6. EI-MS calculated for $C_{16}H_{10}O_2$: 234.0681; observed: 234.0676. $R_f = 0.30$ (1:3 EtOAc/hexanes).

*4.8.7. 3-(7-Ethynyl-2-oxo-2H-chromen-3-yl)-acrylic acid ethyl ester (**4b**)*

Obtained in 61% yield over three steps from **4a**. ^{1}H NMR (400 MHz, $CDCl_3$): δ 7.84 (s, 1H), 7.55 (dd, 1H, $^3J = 16.0$ Hz, $^4J = 0.7$ Hz), 7.49 (d, 1H, $^3J = 8.0$ Hz), 7.44 (m, 1H), 7.40 (d, 1H, $^3J = 8.0$ Hz, $^4J = 1.5$ Hz), 7.10 (d, 1H, $^3J = 16.0$ Hz), 4.27 (q, 2H, $^3J = 7.8$ Hz), 3.33 (s, 1H), 1.34 (t, 3H, $^3J = 7.8$ Hz). APT ^{13}C NMR (100 MHz, $CDCl_3$): δ 166.7, 158.5, 152.9, 142.3, 137.3, 128.3, 128.2, 126.5, 124.3, 122.8, 119.9, 119.1, 81.4, 60.7, 60.7, 14.2. EI-MS calculated for $C_{16}H_{12}O_4$: 268.0736; observed: 268.0740. $R_f = 0.34$ (1:3 EtOAc/hexanes).

*4.8.8. 7-(1-Benzyl-1H-[1,2,3]triazol-4-yl)-4-methyl-chromen-2-one (**1c**)*

^{1}H NMR (500 MHz, $CDCl_3$): δ 7.84 (dd, 1H, $^3J = 8.2$ Hz, $^4J = 1.7$ Hz), 7.77 (s, 1H), 7.67 (d, 1H, $^4J = 1.6$ Hz), 7.64 (d, 1H, $^3J = 8.2$ Hz), 7.43–7.34 (m, 5H), 6.29 (s, 1H), 5.61 (s, 2H), 2.45 (s, 3H). APT ^{13}C NMR (125 MHz, $CDCl_3$): δ 160.7, 153.9, 152.0, 146.5, 134.3, 134.1, 129.3, 129.0, 128.2, 125.1, 121.5, 120.5, 119.6, 115.0, 113.6, 54.4, 18.6. Pos-ES-MS calculated for $C_{19}H_{15}N_3O_2Na$: 340.1057; observed: 340.1057 ($[M + Na]^+$). $R_f = 0.68$ (10:1 CH_2Cl_2/MeOH).

*4.8.9. 9-(1-Benzyl-1H-[1,2,3]triazol-4-yl)-1-methyl-benzo[f]chromen-3-one (**2c**)*

^{1}H NMR (500 MHz, $CDCl_3$): δ 9.32 (broad s, 1H), 7.95 (d, 1H, $^3J = 9.0$ Hz), 7.92 (d, 1H, $^3J = 8.0$ Hz), 7.80 (d, 1H, $^3J = 8.0$ Hz), 7.46 (d, 1H, $^3J = 9.0$ Hz), 7.40–7.35 (m, 6H), 6.41 (s, 1H), 3.06 (s, 3H). APT ^{13}C NMR (125 MHz, $CDCl_3$): δ 160.3, 155.1, 154.3, 134.5, 134.5, 133.3, 131.0, 130.6, 130.2, 129.8, 129.2, 128.9, 128.1, 123.1, 121.9, 118.0, 116.6, 114.8, 54.5, 50.9, 26.5. EI-MS calculated for $C_{23}H_{17}N_3O_2$: 367.1321; observed: 367.1319. $R_f = 0.38$ (30:1 CH_2Cl_2/MeOH).

*4.8.10. 8-(1-Benzyl-1H-[1,2,3]triazol-4-yl)-4-methyl-benzo[g]chromen-2-one (**3c**)*

^{1}H NMR (500 MHz, $CDCl_3$): δ 8.29 (s, 1H), 8.09 (s, 1H), 7.99 (s, 2H), 7.84 (s, 1H), 7.73 (s, 1H), 7.45–7.40 (m, 3H), 7.35–7.30 (m, 2H), 6.36 (d, 1H, $^3J = 1.0$ Hz), 5.64 (s, 2H), 2.55 (d, 3H, $^3J = 1.5$ Hz). APT ^{13}C NMR (125 MHz, $CDCl_3$): δ 160.6, 151.7, 150.6, 134.8, 134.4, 130.3, 129.6, 129.3, 129.0, 128.2, 124.9, 123.9, 123.5, 120.3, 120.2, 116.4, 115.8, 113.1, 54.4, 18.7. EI-MS calculated for $C_{23}H_{17}N_3O_2$: 367.1321; observed: 367.1321. $R_f = 0.39$ (30:1 CH_2Cl_2/MeOH).

*4.8.11. 3-[7-(1-Benzyl-1H-[1,2,3]triazol-4-yl)-2-oxo-2H-chromen-3-yl]-acrylic acid ethyl ester (**4c**)*

^{1}H NMR (500 MHz, $CDCl_3$): δ 7.86 (s, 1H), 7.84 (dd, 1H, $^3J = 8.1$ Hz, $^4J = 1.6$ Hz), 7.78 (s, 1H), 7.73 (d, 1H, $^4J = 1.6$ Hz), 7.58 (d, 1H, $^3J = 7.8$ Hz), 7.57 (d, 1H, $^3J = 16.0$ Hz), 7.46–40 (m, 3H), 7.36–7.33

(m, 2H), 7.10 (d, 1H, $^3J = 16.0$ Hz), 5.61 (s, 2H), 4.28 (q, 2H, $^3J = 7.2$ Hz), 1.35 (t, 3H, $^3J = 7.2$ Hz). ^{13}C NMR (125 MHz, $CDCl_3$): δ 166.9, 159.0, 154.1, 154.0, 146.4, 142.9, 137.8, 135.2, 134.2, 129.3, 129.05, 128.98, 128.2, 123.7, 122.1, 120.7, 118.6, 113.1, 60.7, 54.4, 14.3. EI-MS calculated for $C_{23}H_{19}N_3O_4$: 401.1375; observed: 401.1375. $R_f = 0.52$ (30:1 CH_2Cl_2/MeOH).

Acknowledgements

This work was funded by the Natural Sciences and Engineering Research Council of Canada (NSERC), the Alberta Ingenuity Centre for Carbohydrate Science (AICCS), and the University of Alberta. JAK acknowledges support from an NSERC PGS-M scholarship. QKT was supported by an Alberta Ingenuity postdoctoral fellowship. We would like to thank M. Richards for editorial assistance, W. Moffat and the University of Alberta Spectral Services for support, and the Canadian Foundation for Innovation for infrastructure support.

Appendix. Supporting information

Supporting information associated with this article can be found in the online version, at doi: 10.1016/j.dyepig.2009.01.001.

References

[1] Meares C. Editorial: introduction to bioconjugate chemistry. Bioconjugate Chem 1990;1(1):1–2.
[2] Medintz IL, Uyeda HT, Goldman ER, Mattoussi H. Quantum dot bioconjugates for imaging, labelling and sensing. Nat Mater 2005;4(6):435–46.
[3] Hermanson G. Bioconjugate techniques. New York: Academic Press; 1996.
[4] Niemeyer C. Bioconjugation protocols: strategies and methods. New Jersey: Humana Press; 2004.
[5] Kapanidis AN, Weiss S. Fluorescent probes and bioconjugation chemistries for single-molecule fluorescence analysis of biomolecules. J Chem Phys 2002;117(24):10953–64.
[6] Means GE, Feeney RE. Chemical modifications of proteins: history and applications. Bioconjugate Chem 1990;1(1):2–12.
[7] Weiss S. Fluorescence spectroscopy of single biomolecules. Science 1999;283(5408):1676–83.
[8] Prescher JA, Bertozzi CR. Chemistry in living systems. Nat Chem Biol 2005;1(1):13–21.
[9] Rostovtsev VV, Green LG, Fokin VV, Sharpless KB. A stepwise huisgen cycloaddition process: copper(I)-catalyzed regioselective "ligation" of azides and terminal alkynes. Angew Chem Int Ed 2002;41(14):2596–9.
[10] Tornoe CW, Christensen C, Meldal M. Peptidotriazoles on solid phase: [1,2,3]-triazoles by regiospecific copper(I)-catalyzed 1,3-dipolar cycloadditions of terminal alkynes to azides. J Org Chem 2002;67(9):3057–64.
[11] Molteni G. 1,3-Dipolar cycloadditions in aqueous media. Heterocycles 2006;68(10):2177–202.
[12] Tornoe CW, Meldal M. In: Lebl M, Houghten RA, editors. Peptides 2001: proceedings of the American peptide symposium. San Diego: American Peptide Society and Kluwer Academic Publishers; 2001. p. 263–4.
[13] Sen Gupta S, Kuzelka J, Singh P, Lewis WG, Manchester M, Finn MG. Accelerated bioorthogonal conjugation: a practical method for the ligation of diverse functional molecules to a polyvalent virus scaffold. Bioconjugate Chem 2005;16(6):1572–9.
[14] Bock VD, Hiemstra H, van Maarseveen JH. Cu–I-catalyzed alkyne-azide "click" cycloadditions from a mechanistic and synthetic perspective. Eur J Org Chem 2005;1:51–68.
[15] Speers AE, Cravatt BF. Profiling enzyme activities in vivo using click chemistry methods. Chem Biol 2004;11(4):535–46.
[16] Manetsch R, Krasinski A, Radic Z, Raushel J, Taylor P, Sharpless KB, et al. In situ click chemistry: enzyme inhibitors made to their own specifications. J Am Chem Soc 2004;126(40):12809–18.
[17] Xie J, Seto CT. A two stage click-based library of protein tyrosine phosphatase inhibitors. Bioorg Med Chem 2007;15(1):458–73.
[18] Stubbs KA, Scaffidi A, Debowski AW, Mark BL, Stick RV, Vocadlo DJ. Synthesis and use of mechanism-based protein-profiling probes for retaining beta-D-glucosaminidases facilitate identification of *Pseudomonas aeruginosa* NagZ. J Am Chem Soc 2008;130(1):327–35.
[19] Sivakumar K, Xie F, Cash BM, Long S, Barnhill HN, Wang Q. A fluorogenic 1,3-dipolar cycloaddition reaction of 3-azidocoumarins and acetylenes. Org Lett 2004;6(24):4603–6.
[20] Zhou Z, Fahrni CJ. A fluorogenic probe for the copper(I)-catalyzed azide-alkyne ligation reaction: modulation of the fluorescence emission via 3(*n*,pi)-1(pi,pi) inversion. J Am Chem Soc 2004;126(29):8862–3.
[21] Sawa M, Hsu TL, Itoh T, Sugiyama M, Hanson SR, Vogt PK, et al. Glycoproteomic probes for fluorescent imaging of fucosylated glycans in vivo. Proc Natl Acad Sci U S A 2006;103(33):12371–6.
[22] Hsu TL, Hanson SR, Kishikawa K, Wang SK, Sawa M, Wong CH. Alkynyl sugar analogs for the labeling and visualization of glycoconjugates in cells. Proc Natl Acad Sci U S A 2007;104(8):2614–9.
[23] Xie F, Sivakumar K, Zeng QB, Bruckman MA, Hodges B, Wang Q. A fluorogenic 'click' reaction of azidoanthracene derivatives. Tetrahedron 2008;64(13):2906–14.
[24] Sun WC, Gee KR, Haugland RP. Synthesis of novel fluorinated coumarins: excellent UV-light excitable fluorescent dyes. Bioorg Med Chem Lett 1998;8(22):3107–10.
[25] Zhu Q, Uttamchandani M, Li D, Lesaicherre ML, Yao SQ. Enzymatic profiling system in a small-molecule microarray. Org Lett 2003;5(8):1257–60.
[26] Blum MM, Timperley CM, Williams GR, Thiermann H, Worek F. Inhibitory potency against human acetylcholinesterase and enzymatic hydrolysis of fluorogenic nerve agent mimics by human paraoxonase 1 and squid diisopropyl fluorophosphatase. Biochemistry 2008;47(18):5216–24.
[27] Kage KL, Richardson PL, Traphagen L, Severin J, Pereda-Lopez A, Lubben T, et al. A high throughput fluorescent assay for measuring the activity of fatty acid amide hydrolase. J Neurosci Methods 2007;161(1):47–54.
[28] Beatty KE, Liu JC, Xie F, Dieterich DC, Schuman EM, Wang Q, et al. Fluorescence visualization of newly synthesized proteins in mammalian cells. Angew Chem Int Ed 2006;45(44):7364–7.
[29] Seela F, Sirivolu VR, Chittepu P. Modification of DNA with octadiynyl side chains: synthesis, base pairing, and formation of fluorescent coumarin dye conjugates of four nucleobases by the alkyne–azide "click" reaction. Bioconjugate Chem 2008;19(1):211–24.
[30] O'Reilly RK, Joralemon MJ, Hawker CJ, Wooley KL. Fluorogenic 1,3-dipolar cycloaddition within the hydrophobic core of a shell cross-linked nanoparticle. Chemistry 2006;12(26):6776–86.
[31] Valeur B. Molecular fluorescence: principles and applications. Weinheim: Wiley-VCH; 2002.
[32] Adamczyk M, Cornwell M, Huff J, Rege S, Rao TVS. Novel 7-hydroxycoumarin based fluorescent labels. Bioorg Med Chem Lett 1997;7(15):1985–8.
[33] Wu J, Liao Y, Yang Z. Synthesis of 4-substituted coumarins via the palladium-catalyzed cross-couplings of 4-tosylcoumarins with terminal acetylenes and organozinc reagents. J Org Chem 2001;66(10):3642–5.
[34] Valizadeh H, Shockravi A. An efficient procedure for the synthesis of coumarin derivatives using $TiCl_4$ as catalyst under solvent-free conditions. Tetrahedron Lett 2005;46(20):3501–3.
[35] Tao ZF, Qian XH, Fan MC. Regioselective synthesis and photooxygenations of furonaphthopyrones starting from 2,7-naphthalenediol. Tetrahedron 1997;53(39):13329–38.
[36] Kolancilar H, Oyman U. Investigation of the Pechmann reaction between 2,7-dihydroxynaphthalene and ethyl acetoacetate with different condensing agents. Synthesis of benzocoumarin and benzochromone systems and their bi- and bis-derivatives. J Indian Chem Soc 2003;80(9):853–7.
[37] Kolancilar H. Investigation of Pechmann condensation products of ethyl acetoacetate with 2,7-dihydroxynapthalene. Trakya Universitesi Bilimsel Arasturmalar Dergisi 2002;1:7–10.
[38] Padmanabhan S, Peri R, Triggle DJ. Formation of chromenes and coumarin derivatives from salicyladehydes and 2-pentenedioate: facile route to 3-formylcoumarins. Synth Commun 1996;26(4):827–31.
[39] Chinchilla R, Najera C. The sonogashira reaction: a booming methodology in synthetic organic chemistry. Chem Rev 2007;107(3):874–922.
[40] Angell Y, Burgess K. Base dependence in copper-catalyzed Huisgen reactions: efficient formation of bistriazoles. Angew Chem Int Ed 2007;46(20):3649–51.
[41] Key JA, Cairo CW, Ferguson MJ. 7,7′-(3,3′-Dibenzyl-3*H*,3′*H*-4,4′-bi-1,2,3-triazole-5,5′-diyl)bis(4-methyl-2*H*-chromen-2-one). Acta Crystallogr E 2008;64(10):o1910.
[42] Williams ATR, Winfield SA, Miller JN. Relative fluorescence quantum yields using a computer-controlled luminescence spectrometer. Analyst 1983;108(1290):1067–71.
[43] Seixas de Melo JB, Becker RS, Macanita AL. Photophysical behavior of coumarins as a function of substitution and solvent: experimental evidence for the existence of a lowest lying (n,π^*) state. J Phys Chem 1994;98:6054–8.
[44] Casida ME, Jamorski C, Casida KC, Salahub DR. J Chem Phys 1998;108:4439–49.
[45] Dreuw A, Head-Gordon M. Single-reference ab initio methods for the calculation of excited states of large molecules. Chem Rev 2005;105(11):4009–37.
[46] See supporting information for a additional data used in the correlation.
[47] Jacquemin D, Preat J, Wathelet V, Fontaine M, Perpete EA. Thioindigo dyes: highly accurate visible spectra with TD-DFT. J Am Chem Soc 2006;128(6):2072–83.
[48] Lavis LD, Raines RT. Bright ideas for chemical biology. ACS Chem Biol 2008;3(3):142–55.
[49] Gottlieb HE, Kotlyar V, Nudelman A. NMR chemical shifts of common laboratory solvents as trace impurities. J Org Chem 1997;62(21):7512–5.
[50] Perdew JP, Burke K, Ernzerhof M. Generalized gradient approximation made simple. Phys Rev Lett 1996;77(18):3865–8.
[51] Hehre WJ, Radom L, Schleyer PVR, Pople JA. *Ab initio* molecular orbital theory. New York: John Wiley and Sons; 1985.
[52] Frisch MJ, Trucks GW, Schlegel HB, Scuseria GE, Robb MA, Cheeseman JR, et al. Gaussian 03. revision B.05. Pittsburgh, PA: Gaussian Inc.; 2003.

[53] Cances E, Mennucci B, Tomasi J. A new integral equation formalism for the polarizable continuum model: theoretical background and applications to isotropic and anisotropic dielectrics. J Chem Phys 1997;107(8):3032–41.
[54] Cossi M, Scalmani G, Rega N, Barone V. New developments in the polarizable continuum model for quantum mechanical and classical calculations on molecules in solution. J Chem Phys 2002;117(1):43–54.
[55] Alvarez SG, Alvarez MT. A practical procedure for the synthesis of alkyl azides at ambient temperature in dimethyl sulfoxide in high purity and yield. Synthesis (Stuttg) 1997;4:413–4.
[56] Timerghazin QK, Carlson HJ, Liang C, Campbell RE, Brown A. Computational prediction of absorbance maxima for a structurally diverse series of engineered green fluorescent protein chromophores. J Phys Chem B 2008;112(8):2533–41.